THE JOURNAL OF PHYSICAL CHEMISTRY B

Article

pubs.acs.org/JPCB

Glass Forming Ability and Alloying Effect of a Noble-Metal-Based Glass Former

Luis G. V. Gonçalves, Cláudio J. DaSilva,* and José P. Rino

Departamento de Física, Universidade Federal de São Carlos, 13.565-905, São Carlos, São Paulo, Brazil

ABSTRACT: This work addresses the question on how the glass-forming ability (GFA) of a binary Pd−Ni metallic glass can be enhanced by the alloying effect of Pt. The structural features and slow dynamics of liquid and glassy states on both alloys are investigated by molecular dynamics simulations. Both alloys show typical features of glassy dynamics, namely, the non-Arrhenian behavior of diffusion and relaxation and the fractional Stokes−Einstein relation validity at low temperatures. On the basis of the analysis of the dynamical susceptibilities, we demonstrate that there is a strong influence of the alloying effect on the collective motion of the species, revealing that the GFA of the binary liquid increases with Pt alloying.

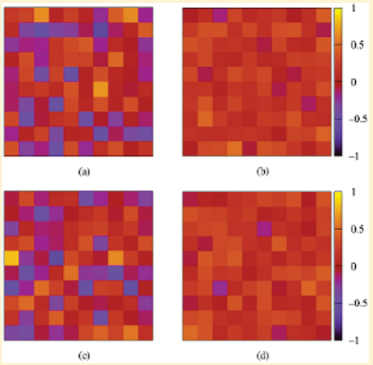

INTRODUCTION

Since the discovery of amorphous metallic alloys by Klement and Duwez,[1,2] noble-metal-based bulk metallic glasses (BMGs) have drawn increasing interest due to their extremely high glass forming ability (GFA) and their superior mechanical performance under extreme external conditions. Some exceptional systems such as Pd−Ni−P and Pt−Cu−Ni−P were observed with a very low critical cooling rate for glass formation[3] (on the order of 0.1 K/s) and with large global plasticity.[4] Nishiyama and colleagues have reported that the replacement of Pd by Pt in Ni-free $Pd_{40}Cu_{40}P_{20}$ enables the development of a glass-forming alloy with the largest GFA to date,[5] with an extremely low critical cooling rate of 0.05 K/s. Very recently, a Pt-based $Pt_{57.5}Cu_{14.5}Ni_5P_{22.5}$ BMG reported by Carmo et al. presented a surprising durability when used to boost performance in electrochemical devices.[6] Another important achievement was accomplished by Demetriou et al. They created a remarkable Pd-based metallic glass whose combination of high yield strength and high toughness establishes the composition $Pd_{79}Ag_{3.5}P_6Si_{9.5}Ge_2$ as the material with the highest damage tolerance known to date.[7]

The outstanding features of the aforementioned BMGs were achieved by favoring the glass formation, and consequently the critical sample diameters, through the accurate selection of alloy compositions at deep eutectic. Many criteria have been proposed to improve the GFA of multicomponent metallic systems. Several authors have shown that the addition of a third element that exhibits different properties, such as atomic size and crystalline symmetry, to binary metallic alloys can dramatically improve the ease of glass formation.[8−11] Therefore, it is clear that the roles of minor additions in the formation of BMGs is fundamental to optimize the properties of the alloys.[12] In this regard, the present work focuses on the glassy dynamics of two Pd−Ni based metallic systems (namely, the $Pd_{45}Ni_{55}$ and $Pd_{35}Pt_{10}Ni_{55}$ compositions) and their ability to form a glassy alloy. Specifically, we investigated the effects of the addition of 10% of Pt on the Pd−Ni binary system and its consequence on the GFA. These two systems are particularly interesting because the addition of a small amount of phosphorus on them increases their strength-to-weight ratio, thus having a great scientific and technological interest.[13]

SIMULATION DETAILS

To address slow dynamics features and structural evolution during the liquid−glass transition in both alloys, we employed the LAMMPS open code software for molecular dynamics simulation.[14] For both alloys, we set up systems with 8000 particles inside a cubic box under periodic boundary conditions in all directions. The particles interact via the embedded-atom method (EAM) potential.[15] The data set for the functions of the EAM we adopted here was originally developed to fit properties of single component metallic systems obtained from experiment and density functional theory calculations. The pair interaction functions between distinct species were built using the geometric mean of the single species pair interactions.[16]

The atomic configurations for both alloys were created by setting up all particles in random positions. We applied a minimization run via the conjugate gradient technique to eliminate overlapping of atoms. We then allowed the systems to thermalize at any desired temperature, and the dynamical properties were calculated in the supercooled regime. During thermalization, the simulation box was relaxed isotropically in a constant-pressure ensemble while keeping its cubic shape. After adequate thermalization, the diffusion coefficient was calculated

Received: August 25, 2011
Revised: December 27, 2011
Published: December 28, 2011

   dx.doi.org/10.1021/jp208244n | *J. Phys. Chem. B* 2012, 116, 1356−1359

using the Einstein relation $D = \lim_{t\to\infty}(1/6t)\langle r_i^2(t)\rangle$, where $\langle r_i^2(t)\rangle$ is the mean-square displacement for the ith species. The alpha-relaxation time τ_α was obtained from the intermediate scattering function given by

$$F_s(\vec{q}, \vec{r}(t)) = \frac{1}{N}\sum_{i=1}^{N}\cos[\vec{q}\cdot(\vec{r}_i(t) - \vec{r}_i(0))] \quad (1)$$

where $\vec{q}$ was chosen as the first sharp peak of the static structure factor. This function gives us a suitable definition of the characteristic relaxation time for liquids.[17] The definition of τ_α adopted here is via fitting of F_s by the function $\exp(-t/\tau_\alpha)^\beta$. Both D and τ_α were calculated for 10 distinct initial configurations in a canonical ensemble. This sampling procedure is crucial for the calculation of all dynamical properties to average out fluctuations and to estimate uncertainties.

RESULTS AND DISCUSSION

We begin by considering the dynamical properties of the binary and ternary metallic liquids approaching the glass transition. According to Table 1, there is a single diffusion regime, meaning that all element diffusivities present very similar temperature dependences in each composition. The addition of Pt decreases in less than 4% the high temperature activation energy E_A of Pd and Ni. The relaxation in the low temperature regime ($T \leq 1000$ K) was fitted with an inverse power law $\tau_\alpha \propto (T - T_c)^{-\lambda}$, according to the mode-coupling theory (MCT).[18] It is well-known that higher values of λ are associated with lower fragility of the supercooled liquid and hence an increased GFA. Our results show that the exponent λ changed from 2.25 for the binary alloy to 2.50 for the ternary one. This is a first indication of the alloying effect of Pt in $Pd_{45}Ni_{55}$ on its GFA. In Figure 1, one can see that both alloys are characterized as fragile glass formers because of their non-Arrhenian behavior of relaxation. The values of τ_α were fitted with the Vogel–Fulcher–Tammann (VFT) function[19] for all temperatures: $\tau_\alpha = \tau_0 \exp[D_f T_0/(T - T_0)]$. This equation suggests a divergence of the relaxation time at a finite temperature T_0. It should be noted that a smaller value of the parameter D_f (referred to as the "fragility parameter") corresponds to a more fragile glass. Our values of D_f shown in Table 1 reveal that the glass former $Pd_{35}Pt_{10}Ni_{55}$ is less fragile than $Pd_{45}Ni_{55}$.

Another interesting characteristic of these systems is the fact that they present a breakdown of the Stokes–Einstein (SE) relation. More specifically, they obey the fractional Stokes–Einstein relation $D \propto (\eta/T)^{-\xi}$ for low temperatures, a very common feature among fragile glass formers.[20−22] The values of ξ are generally observed in the range 0.5−0.8. $\xi = 1$ corresponds to the SE relation. The fractional SE relation is believed to be related to the development of spatially heterogeneous regions in liquids when the temperature decreases[23] and, consequently, to their GFA. As can be seen in Figure 2, the exponent ξ changes from 0.72(4) to 0.95(1) for the binary $Pd_{45}Ni_{55}$ alloy at approximately 1000 K. In its turn, for the ternary $Pd_{35}Pt_{10}Ni_{55}$ alloy, ξ changes from 0.74(1) to 0.97(2). The values of ξ are very similar for both alloys, indicating that the growing of short-range order structures in the supercooled liquids is almost the same (as we will show latter in the paper).

Table 1. Results of Fits on Diffusion and Relaxation for Both Alloys[a]

	$Pd_{45}Ni_{55}$		$Pd_{35}Pt_{10}Ni_{55}$		
	Pd	Ni	Pd	Ni	Pt
D_0 (Å^2/ps)	8.0(3)	8.2(4)	6.56(9)	6.96(4)	6.04(13)
E_A (eV)	0.440(5)	0.434(6)	0.422(2)	0.422(9)	0.426(3)
D_f	1.61(11)	1.79(13)	1.68(7)	1.82(7)	1.54(6)
T_0 (K)	647(11)	636(12)	645(8)	637(9)	655(7)
λ	2.25(5)			2.50(5)	
T_c (K)	760(10)			750(10)	

[a]For $T \geq 1400$ K, $D(T) = D_0 \exp(-E_A/k_B T)$. For all temperatures, $\tau_\alpha \propto \exp[D_f T_0/(T - T_0)]$. For $T \leq 1000$ K, $\tau_\alpha \propto (T - T_c)^{-\lambda}$.

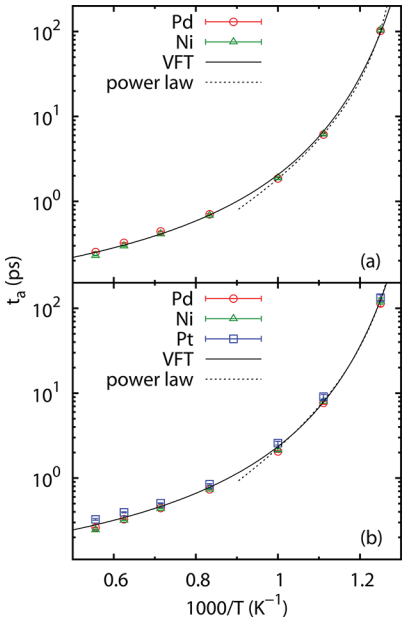

Figure 1. Structural relaxation time as a function of temperature of all species for (a) $Pd_{45}Ni_{55}$ and (b) $Pd_{35}Pt_{10}Ni_{55}$ alloys. Average fits of VFT-function and power law are also shown.

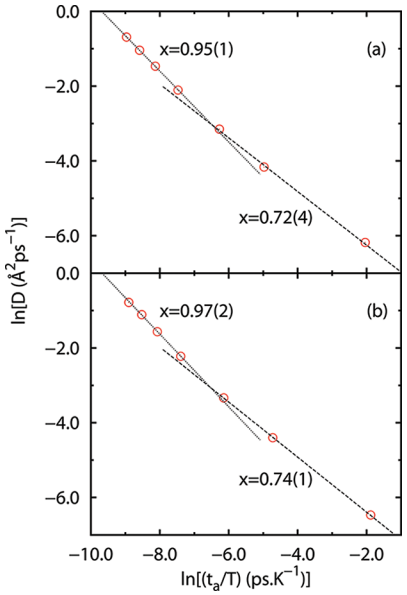

Figure 2. The log × log plot of D vs τ_α/T for Ni atoms in (a) $Pd_{45}Ni_{55}$ and (b) $Pd_{35}Pt_{10}Ni_{55}$.

dx.doi.org/10.1021/jp208244n | J. Phys. Chem. B 2012, 116, 1356–1359

Strong evidence for the GFA enhancement of the binary alloy with the addition of Pt can be observed by analyzing the dynamic susceptibility[19,24]

$$\chi_4(t) = N[\langle F_s^2(\vec{q}, \vec{r}(t))\rangle - \langle F_s(\vec{q}, \vec{r}(t))\rangle^2] \quad (2)$$

This quantity provides information about the degree of spatial cooperativeness in glass forming liquids. The peak of χ_4 indicates at what time interval the dynamics becomes more cooperative, and its height is associated with the dynamical correlation length.[25] Figure 3 shows the behavior of χ_4 as a function of time, revealing that in both alloys the dynamics is strongly correlated and heterogeneous. One can see that the alloying effect of Pt in the binary glass former clearly increases the peak height of χ_4. The inset of Figure 3 shows a considerable change in the total relaxation between both alloys. These results show that the atomic motion in $Pd_{35}Pt_{10}Ni_{55}$ is more cooperative than that in $Pd_{45}Ni_{55}$, which characterizes the improvement of the GFA of the binary alloy upon the addition of Pt.

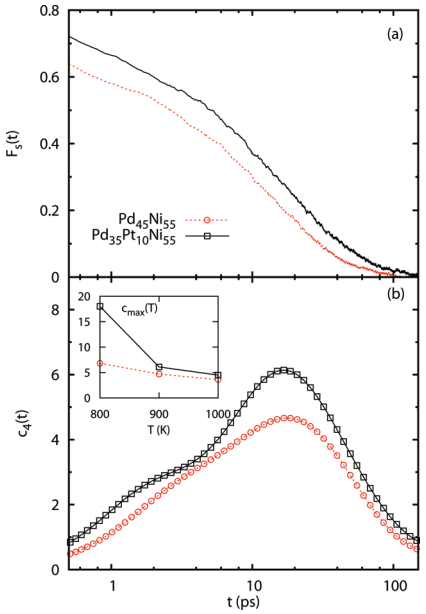

Figure 3. (a) Self-intermediate scattering function at 900 K for both alloys. (b) Dynamical susceptibility χ_4 as a function of time at the same temperature. The inset shows the dependence with the temperature of the maximum of χ_4.

Another very important factor in determining the enhancement of the GFA is the stability of the dynamical correlation length with temperature.[19] We analyzed the behavior of χ_4 for different temperatures approaching the glass transition for both binary and ternary alloys. We found that the maximum of χ_4 shifts to larger times and has a larger value when T is decreased, revealing the increasing length scale of dynamic heterogeneity. Furthermore, the increasing of the maximum is much more pronounced for the alloy with added Pt (see inset in Figure 3). This is more clear evidence that the addition of Pt enhanced the GFA of the binary supercooled metallic liquid.

Furthermore, we quantified the short-range order structure of both liquid and glassy phases. Starting from a liquid in thermal equilibrium at 2000 K in the NPT ensemble (with zero pressure), we cooled both systems at a 20 K/ns rate down to 200 K. From the diagram of the volume against temperature, we evaluated the fictive temperature of both systems equal to 750 K. The fictive temperature is usually associated as an estimate for the glass transition temperature in simulations. The configurations were monitored periodically during the cooling path using the common neighbor parameter (CNP)[26,27] to provide information about the atomic packing. This method establishes relationships between a given particle and all its nearest neighbors in order to identify local ordered structures, such as coordination polyhedra. It is confirmed by experiments that the predominant polyhedra present in metallic glasses are icosahedral.[28] We first analyzed the nearest-neighbor environment around the smaller species (Ni). As can be seen in Figure 4, there is a sharp increase in the number of Ni-centered icosahedra toward the glass transition region. This is associated with the increase of viscosity that leads to glass formation. The average atomic coordination around Ni is also shown in Figure 4, reinforcing the icosahedral order of Ni. The alloying effect of Pt regarding local structure is relatively weak, namely, a decrease of roughly 4% on the number of icosahedra in the Pt-added glass structure. However, the CNP analysis did not detect any special structures around Pd or Pt atoms. This could be related with the fact that the fraction of polyhedra in BMGs is a composition dependent property, as confirmed by Cheng et al. using computer simulation.[9] In order to show structural inhomogeneities in our MD model, we mapped the density of Pt and Pd atoms at two different planes for the glassy phase of the ternary alloy at 200 K. Figure 5 shows that the spatial distribution of the atoms is homogeneous for Pd and inhomogeneous for Pt. One may note that there is a certain stringed Pt atom chain; however, there is no special structure centered at Pt, as confirmed by the CNP analysis.

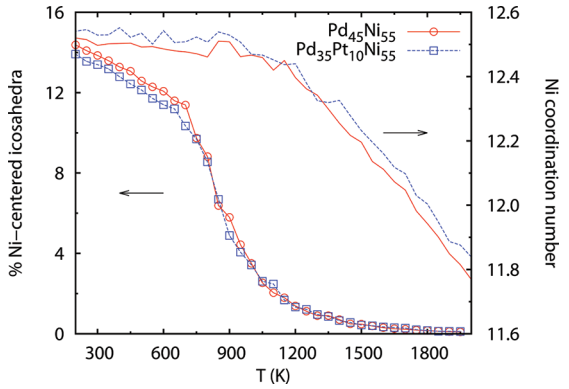

Figure 4. The fraction of Ni-centered clusters whose coordination is icosahedral for the two Pd-based glasses. The fraction rises appreciably on cooling toward the glass transition temperature T_g.

CONCLUDING REMARKS

In summary, we were able to characterize the glass forming ability of two Pd-based metallic melts. The model used in this work was suitable for simulating the main features of the dynamical behavior found in typical glass forming alloys. Our results for the dynamical properties show that both alloys are fragile glass-formers and obey the fractional Stokes−Einstein relation for low temperatures. The Pt-added alloy presented a mild increase in the relaxation time. The change in the dynamic susceptibility with the addition of Pt in the binary alloy revealed stronger evidence for the improvement of its glass forming ability. Moreover, the structural evolutions of both liquids upon

dx.doi.org/10.1021/jp208244n | J. Phys. Chem. B 2012, 116, 1356−1359

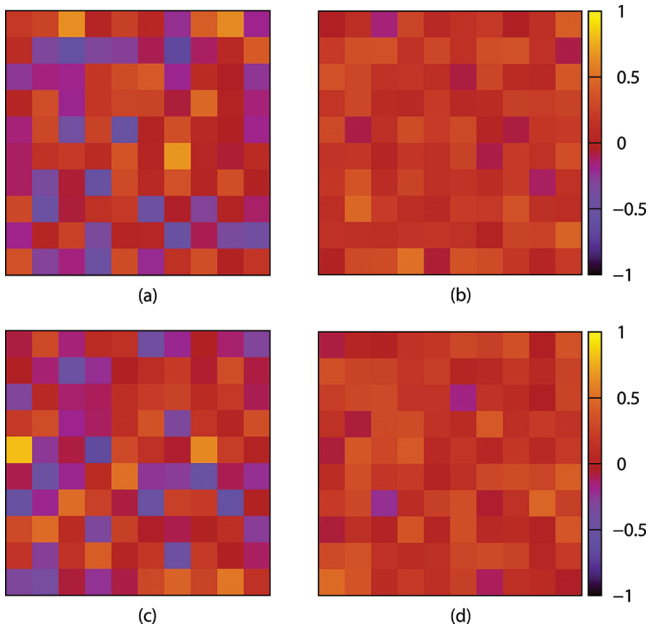

Figure 5. Density mapping on the *xz*-plane (a and b) and on the *xy*-plane (c and d) for the Pd−Ni−Pt glass at 200 K. Left plots refer to the density of Pt and right ones to the density of Pd. The scale indicates the deviation from the average in-plane density of each species.

cooling, which are characterized by the increasing number of Ni-centered icosahedra, are very similar. Overall, this study illustrates in an unambiguous fashion the chief processes responsible for the enhancement of the glass forming ability in this family of bulk metallic glasses.

AUTHOR INFORMATION

Corresponding Author

*E-mail: clauz@df.ufscar.br.

ACKNOWLEDGMENTS

The authors would like to thank the Coordenação de Aperfeiçoamento de Pessoal de Nível superior (CAPES), the Conselho Nacional de Desenvolvimento Científico e Tecnológico (CNPq), and the Fundação de Amparo à Pesquisa do Estado de São Paulo (FAPESP) for financial support.

REFERENCES

(1) Klement, W.; Willens, R. H.; Duwez, P. *Nature* **1960**, *187*, 869−870.
(2) Duwez, P.; Willens, R. H.; Crewdson, R. C. *J. Appl. Phys.* **1965**, *36*, 2267.
(3) He, Y.; Schwarz, R. B.; Archuleta, J. I. *Appl. Phys. Lett.* **1996**, *69*, 1861.
(4) Schroers, J.; Johnson, W. L. *Phys. Rev. Lett.* **2004**, *93*, 255506.
(5) Nishiyama, N.; Takenaka, K.; Inoue, A. *Appl. Phys. Lett.* **2006**, *88*, 121908.
(6) Carmo, M.; Sekol, R. C.; Ding, S.; Kumar, G.; Schroers, J.; Taylor, A. D. *ACS Nano* **2011**, *5*, 2979.
(7) Demetriou, M. D.; Launey, M. E.; Garrett, G.; Schramm, J. P.; Hofmann, D. C.; Johnson, W. L.; Ritchie, R. O. *Nat. Mater.* **2011**, *10*, 123−128.
(8) Zeng, Y.; Inoue, A.; Nishiyama, N.; Chen, M. *Intermetallics* **2010**, *18*, 1790.
(9) Cheng, Y. Q.; Ma, E.; Sheng, H. W. *Appl. Phys. Lett.* **2008**, *83*, 111913.
(10) Cheng, Y. Q.; Ma, E.; Sheng, H. W. *Phys. Rev. Lett.* **2009**, *102*, 245501.
(11) Fujita, T.; Konno, K.; Zhang, W.; Kumar, V.; Matsuura, M.; Inoue, A.; Sakurai, T.; Chen, M. W. *Phys. Rev. Lett.* **2009**, *103*, 075502.
(12) Wang, W. H. *Prog. Mater. Sci.* **2007**, *52*, 540−596.
(13) Suryanarayana, C.; Inoue, A. *Bulk Metallic Glasses*; CRC Press: New York, 2011.
(14) Plimpton, S. *J. Comput. Phys.* **1995**, *117*, 1−19.
(15) Foiles, S. M.; Baskes, M. I.; Daw, M. S. *Phys. Rev. B* **1986**, *33*, 7983.
(16) Daw, M. S.; Baskes, M. I. *Phys. Rev. Lett.* **1983**, *50*, 1285.
(17) Heuer, A. *J. Phys.: Condens. Matter* **2008**, *20*, 373101.
(18) Gotze, W.; Sjogren, L. *Rep. Prog. Phys.* **1992**, *55*, 241−376.
(19) Berthier, L.; Biroli, G. *Rev. Mod. Phys.* **2011**, *83*, 587−645.
(20) Tanaka, H. *Phys. Rev. E* **2003**, *68*, 011505.
(21) Harris, K. R. *J. Chem. Phys.* **2009**, *131*, 054503.
(22) Zhu, A.; Shiflet, G. J.; Poon, S. J. *Phys. Rev. B* **2010**, *81*, 224209.
(23) Chathoth, S. M.; Samwer, K. *Appl. Phys. Lett.* **2010**, *97*, 221910.
(24) Fujita, T.; Guan, P. F.; Sheng, H. W.; Inoue, A.; Sakurai, T.; Chen, M. W. *Phys. Rev. B* **2010**, *81*, 140204.
(25) Keys, A. S.; Abate, A. R.; Glotzer, S. C.; Durian, D. J. *Nat. Phys.* **2007**, *3*, 260−264.
(26) Tsuzuki, H.; Branicio, P. S.; Rino, J. P. *Comput. Phys. Commun.* **2007**, *177*, 518−523.
(27) Faken, D.; Jonsson, H. *Comput. Mater. Sci.* **1994**, *2*, 279−286.
(28) Lee, G. W.; Gangopadhyay, A. K.; Kelton, K. F.; Hyers, R. W.; Rathz, T. J.; Rogers, J. R.; Robinson, D. S. *Phys. Rev. Lett.* **2004**, *93*, 037802.